7. CARRAGEENAN BEADS

7.1. Carrageenan-Amylase Beads

7.1.1. MATERIALS

Potassium dihydrogen phosphate, sodium hydroxide, hydrochloric acid (Qualigens Fine Chemicals, Mumbai, India) and soluble starch (Himedia Laboratories Pvt. Ltd., Mumbai, India) were used as received. Fungal α-amylase, κ-carrageenan (obtained from Irish moss, *Chondrus Crispus*) , potassium chloride, iodine, and potassium iodide were purchased from S. D. Fine-Chem Ltd., Mumbai, India. All the other chemicals and solvents were of analytical grade and were used without further purification. Deionized double-distilled water was used throughout the study.

7.1.2. CHARACTERIZATION OF CARRAGEENAN

The carrageenan procured was derived from Irish moss (*Chondrus Crispus*), which is known to contain kappa (gelling fraction) and lambda (non-gelling fraction) carrageenan as major constituents. Carrageenan sample was tested according to the identification test B (gel constancy test) and D (FTIR study) of USP-27 NF-22, and was found to be kappa-carrageenan with non-gelling fraction (lambda-carrageenan) of less than 5 percent. Moreover, the kappa-carrageenan was confirmed by observing the syneresis phenomenon, which is not observed with iota-carrageenan gels. Particle size of carrageenan was determined with the laser diffraction particle size analyzer (MAN 0244/

HYDRO 2000 SM, Malvern Instruments Ltd., UK) using acetonitrile as a vehicle and was found to contain 90% particle of the size less than 156.96 μm. Particle density was determined by liquid displacement method using benzene and was found to be 0.89 g/cm^3. Viscosity of the 1.5% solution in deionized distilled water at 25°C was calculated using Oswald viscometer and was found to be 40 cp.

7.1.3. PREPARATION OF BEADS

Concentrated κ-carrageenan solution in distilled water was prepared by heating the powder dispersion at 70°C to get homogenous solution and cooled to 40°C. Required quantity of enzyme (200 mg α-amylase in 50 ml of final κ-carrageenan solution) was dissolved in small quantity of water and mixed with concentrated κ-carrageenan solution. Final concentration of κ-carrageenan was adjusted in the range of 2.5-3.5% w/v and was used after being degassed under vacuum. The beads were prepared by dropping the κ-carrageenan solution (10 ml) containing α-amylase from the dropping device such as syringe with 18G×½" flat-tip hypodermic needle to a magnetically stirred potassium chloride solution (40 ml) at a rate of 5 ml/min and were allowed to harden for specific time. Different levels (Table 7.1) of κ-carrageenan, potassium chloride and hardening time were selected. The beads were collected by decanting potassium chloride solution, washed with deionized water and dried to a constant weight in vacuum desiccator (Tarsons Products Pvt. Ltd., Kolkata, India) at room temperature for 48 hours.

Table 7.1: Process variables and their levels for 3^3 full factorial design.

Factors	Coded levels	Actual levels
A: κ-Carrageenan concentration (%w/v)	-1	2.5 % w/v
	0	3.0 % w/v
	1	3.5 % w/v
B: Potassium chloride concentration (M)	-1	0.3 M
	0	0.5 M
	1	0.7 M
C: Hardening Time (min)	-1	10 min
	0	20 min
	1	30 min

7.1.4. FACTORIAL DESIGN

Before the application of the design, number of preliminary trials were conducted by changing one variable at a time and keeping other variables fixed to determine the conditions at which the process resulted to beads. In the present study three-level full factorial design (FFD) was employed to generate response surfaces. To determine the experimental error, the experiment at the centre point was repeated five times at different days. The mean % entrapment, T_{50}, T_{90}, and particle size at the center-replicated points were 73.96±0.46%, 33.64±0.65 min, 44.12±1.21 min, and 1.92±0.008 mm respectively and showed good reproducibility of the process. The quadratic coefficients were estimated using the least-squares multiple regression to the observed response. The analysis of variance (ANOVA) was performed in order to determine significance of the fitted equation. All analytical treatments were supported by NCSS software. The process variables with their coded experimental values and the results of the responses are reported in Table 7.2.

Table 7.2: Factorial 3^3: matrix of the experiments and results for the measured responses and the composite index.

ES[a]	Factors/levels			Responses				Transformed		Comp-osite Index (CI)
	Carrag-eenan (% w/v)	KCl (M)	Harde-ning Time (min)	% Immobi-lization	T_{50}	T_{90}	Particle Size ± SD[b] (mm)	% Immobi-lization	T_{90}	
9	-1	-1	-1	65.34	17.15	25.50	1.83±0.19	19.85	50.00	19.85
13	-1	-1	0	62.40	19.20	29.70	1.80±0.17	15.28	45.71	19.57
2	-1	-1	1	60.29	22.10	33.65	1.76±0.18	11.99	41.67	20.32
24	-1	0	-1	62.11	22.30	32.50	1.68±0.20	14.82	42.84	21.98
17	-1	0	0	59.25	25.45	38.60	1.65±0.19	10.37	36.61	23.77
6	-1	0	1	57.24	29.10	44.10	1.61±0.20	7.24	30.98	26.26
1	-1	1	-1	57.27	28.86	42.35	1.63±0.19	7.29	32.77	24.52
27	-1	1	0	54.49	32.65	46.10	1.60±0.20	2.96	28.94	24.02
10	-1	1	1	52.59	36.40	49.70	1.56±0.17	0.00	25.26	24.74
23	0	-1	-1	78.79	24.50	35.30	2.09±0.20	40.80	39.98	50.82
8	0	-1	0	75.97	28.75	41.10	2.06±0.16	36.41	34.05	52.36
15	0	-1	1	73.96	33.05	46.05	2.02±0.17	33.28	28.99	54.29
12	0	0	-1	76.65	30.75	41.50	1.95±0.20	37.46	33.64	53.82
26	0	0	0	73.92	33.70	44.15	1.92±0.19	33.21	30.93	52.28
19	0	0	1	72.02	37.75	50.90	1.88±0.20	30.26	24.03	56.23
3	0	1	-1	70.68	37.86	50.83	1.90±0.22	28.17	24.10	54.07
18	0	1	0	68.00	42.05	55.20	1.87±0.19	24.00	19.63	54.36
21	0	1	1	66.18	44.60	62.95	1.83±0.18	21.16	11.71	59.45
4	1	-1	-1	84.70	31.50	45.40	2.43±0.19	50.00	29.65	70.35
25	1	-1	0	82.02	35.90	49.30	2.41±0.19	45.83	25.66	70.16
11	1	-1	1	80.13	40.95	56.20	2.38±0.18	42.88	18.61	74.27
22	1	0	-1	82.30	38.47	51.90	2.29±0.17	46.26	23.01	73.26
14	1	0	0	79.79	42.10	56.05	2.27±0.19	42.35	18.76	73.59
7	1	0	1	78.03	45.50	62.00	2.24±0.19	39.61	12.68	76.93
5	1	1	-1	77.80	45.60	60.50	2.26±0.18	39.26	14.21	75.04
16	1	1	0	75.42	48.30	67.80	2.24±0.18	35.55	6.75	78.80
20	**1**	**1**	**1**	**73.79**	**51.40**	**74.40**	**2.21**±0.18	**33.01**	**0.00**	**83.01**

[a] ES, experimental sequence.
[b] SD, standard deviation (n=50).

7.1.5. COMPOSITE INDEX

On completion of the individual experiments, a weighted composite index was used to designate a single score utilizing two responses, i.e., % entrapment, and T_{90}. Many researchers have utilized the technique of multiple responses for optimization studies. Derringer and Suich illustrated how several response variables can be transformed into

one response (Derringer and Suich, 1980). The applications of one-sided transformations are also demonstrated by different researchers (Bodeam and Leucata, 1997; Gohel et al., 2003). The application of generalized distance function to incorporate several objectives into a single function has been reported (Shigeo et al., 1994). As the relative contribution of each individual constraint to the "true" composite score was unknown, a decision was made to assign an arbitrary value of one-half to each of the two response variables (Taylor et al., 2000). The empirical composite index was devised to yield a score 100 for an optimum result for each of the two responses and each formulation result was transformed to a value between 0 and 50. For % entrapment, highest value (84.7) was assigned a score equal to 50, and lowest value (52.59) was assigned zero score. For T_{90}, lowest value (25.5) was assigned to zero score and the highest value (74.4) was assigned to 50. The batch having the highest composite index would be considered as a batch fulfilling the desired criteria. The raw data transformations were as follows:

Eq. 7.1 $$\text{Transformed value of \% entrapment or } T_{90} = \frac{Y_i - Y_{min}}{Y_{max} - Y_{min}} \times 50$$

where Y_i is the experimental value of individual response variable, Y_{max} and Y_{min} are maximum and minimum values of individual response variable, respectively.

Eq. 7.2 $$\text{Composite index} = \begin{pmatrix}\text{transformed value}\\ \text{of \% entrapment}\end{pmatrix} + \begin{pmatrix}\text{transformed}\\ \text{value of \% } T_{50}\end{pmatrix}$$

7.1.6. CURVE FITTING

The *'in vitro'* release pattern was evaluated to check the goodness of fit to the zero-order release kinetics (Eq. 7.3), first-order release kinetics (Gibaldi and Feldman, 1967; Wagner, 1969) (Eq. 7.4), Higuchi's square root of time equation (Higuchi, 1963) (Eq. 7.5), Korsmeyer-Peppas' power law equation (Korsmeyer et al., 1983a; Peppas, 1985)

(Eq. 7.6), and Hixson-Crowell's cube root of time equation (Hixson and Crowell, 1931) (Eq. 7.7). The goodness of fit was evaluated by r (correlation coefficient) values. For better understanding residual analysis (Pather et al., 1998) of above models was performed on the optimized formulation.

Eq. 7.3 $$Q_t = Q_0 + K_0 t$$

where Q_t is the amount of drug dissolved in time t, Q_0 is the initial amount of drug in the solution (most times, Q_0=0), K_0 is the zero order release constant and t is release time.

Eq. 7.4 $$Q_t = Q_0 e^{-K_1 t}$$

Where Q_t is the amount of drug dissolved in time t, Q_0 is the initial amount of drug in the solution, K_1 is the first order release constant and t is release time.

Eq. 7.5 $$Q_t = K_H \sqrt{t}$$

where Q_t is the amount of drug dissolved in time t, K_H is the Higuchi dissolution constant and t is release time.

Eq. 7.6 $$Q_t / Q_\infty = K_k t^n$$

where Q_t is the amount of drug dissolved in time t, Q_∞ is the amount of drug dissolved in ∞ time (the drug loaded in the formulation), Q_t / Q_∞ is the fractional release of the drug in time t, K_k is a constant incorporating structural and geometric characteristic of dosage form, n is the release (diffusional) exponent that depends on the release mechanism and the shape of the matrix tested (Ritger and Peppas, 1987) and t is release time. Interpretation of diffusional exponent is given in Table 7.3.

Table 7.3: Interpretation of Korsmeyer-Peppas power law release exponent.

Release exponent (n)	Drug transport mechanism	Rate as a function of time
0.5	Fickian diffusion	$t^{-0.5}$
0.5<n<1.0	Anomalous transport	t^{n-1}
1.0	Case-II transport	Zero order release
Higher than 1.0	Super Case-II transport	t^{n-1}

Eq. 7.7 $$Q_0^{1/3} - Q_t^{1/3} = K_s t$$

where Q_0 is the initial amount of drug in the pharmaceutical dosage form, Q_t is the remaining amount of drug in pharmaceutical dosage form at time t, K_s is a constant incorporating the surface-volume relation and t is release time.

In order to understand the release mechanism, the release data of the optimized batch was fitted to empirical equations proposed by Kopcha (Kopcha et al., 1991) (Eq. 7.8),

Eq. 7.8 $$M = At^{1/2} + Bt$$

In the above equations, M ($\leq$ 70%) is the percentage of drug released at time t, while A and B are, respectively, diffusion and erosion terms. According to this equation, if diffusion and erosion ratio, A/B=1, then the release mechanism includes both diffusion and erosion equally. If A/B>1, then diffusion prevails, while for A/B<1, erosion predominates.

7.1.7. CHARACTERIZATION OF BEADS

7.1.8. ESTIMATION OF A-AMYLASE (DEXTRINOGENIC ASSAY)

The iodine test of Smith and Roe (Smith and Roe, 1957; Hsiu et al., 1964) was modified as follows: Two ml of a 0.2% starch solution was added to 1.0 ml of enzyme diluted in 0.05 M phosphate buffer pH 6.8. The mixture was incubated for 3 minutes at 25° and then reaction was stopped with 1 ml of 1 N HCl. Finally, 20 ml of water and 0.5 ml of 0.01 N iodine solution prepared according to Rice (Rice, 1959) were added and the absorbance A was recorded on a spectrophotometer (Shimadzu UV-1601, Japan) at 660 nm. The

instrument was adjusted to zero reading with iodine blank containing neither enzyme nor substrate. The dextrinogenic activity is expressed in arbitrary units as follows:

Eq. 7.9 $$D = [(A_B - A)/A_B] \cdot E$$

Where A_B is the absorbance of the starch-iodine complex in the absence of enzyme and E is the enzyme dilution. Best results were obtained when the enzyme solution was diluted in such a manner as to make the ratio $(A_B - A)/A_B$, approach 0.20-0.25.

7.1.9. DETERMINATION OF ENTRAPMENT EFFICIENCY

Entrapment efficiency was determined by dissolving the enzyme loaded beads in a magnetically stirred simulated gastric fluid (SGF) without enzyme (USP XXVI) for about 90 min. An aliquot of 2 ml was taken and neutralized to pH 6.8 using 0.01 N sodium hydroxide. The resulting solution was centrifuged at 2500 rpm for 10 min (Remi Instruments Ltd, Mumbai, India) and supernatant was assayed (n=3) for enzyme content by dextrinogenic assay as above. Entrapment efficiency was calculated as:

Eq. 7.10 $$\text{Entrapment efficiency} = \frac{\text{Enzyme loaded}}{\text{Theoretical enzyme loading}} \times 100$$

7.1.10. DETERMINATION OF T50 AND T90

Time required for 50 (T_{50}) and 90 (T_{90}) percent of enzyme release were used to evaluate the onset and duration of action respectively. For optimization purpose, dissolution study of all batches was carried out in 500 ml of SGF without enzyme using the USP XXVI dissolution apparatus 2 (TDT-60T, Electrolab, Mumbai, India) at 37±0.5 °C with paddle speed of 75 rpm. Accurately weighed samples (n=3) equivalent to about 40 mg of α-amylase were subjected to dissolution and aliquots of 2 ml were collected, neutralized to

pH 6.8 using 0.01 N sodium hydroxide, and assayed at 0, 5, 10, 15, 20, 30, 45, 60, 90 and 120 min. T_{50} and T_{90} were found by extrapolating the % enzyme released versus time plot.

7.1.11. PARTICLE SIZE MEASUREMENTS

The particle sizes of 50 gel beads were measured with a gauge type micrometer (0.05 mm least count, Durga Scientific Pvt. Ltd., Vadodara, India) for each formulation and the mean particle size was determined.

7.1.12. FOURIER TRANSFORM INFRA-RED SPECTROSCOPY (FTIR)

IR transmission spectra were obtained using a FTIR spectrophotometer (FTIR-8300, Shimadzu, Japan). A total of 2% (w/w) of sample, with respect to the potassium bromide (KBr; S. D. Fine Chem Ltd., Mumbai, India) disc, was mixed with dry KBr. The powder was compressed into KBr disc under a hydraulic press at 10,000 psi. Each KBr disc was scanned at 4 mm/s at a resolution of 2 cm over a wavenumber region of 400–4000 cm^{-1}.

7.1.13. DIFFERENTIAL SCANNING CALORIMETRY (DSC)

DSC thermograms were obtained using an automatic thermal analyzer system (DSC-60, Shimadzu, Japan). Temperature calibration was performed using indium as a standard. Samples were crimped in a standard aluminum pan and heated from 40 to 400 °C at a heating rate of 10 °C/min under constant purging of dry nitrogen at 30 ml/min. An empty pan, sealed in the same way as the sample, was used as a reference.

7.1.14. SCANNING ELECTRON MICROSCOPY (SEM)

The purpose of SEM study was to obtain a topographical characterization of beads. The beads were mounted on brass stubs using carbon paste. SEM photographs were taken with scanning electron microscope (JSM-5610LV, Jeol Ltd., Japan) at the required magnification at room temperature. The working distance of 39 mm was maintained and acceleration voltage used was 5 kV, with the secondary electron image (SEI) as a detector.

7.1.15. PREPARATION OF CAPSULE FORMULATION & STABILITY STUDY

Accurately weighed carrageenan beads equivalent to 40 mg of α-amylase were filled into a hard gelatin capsule manually. The joint of the capsule body and cap was carefully sealed by pressing them to fit in the lock mechanism. The capsules were packed in high density polyethylene (HDPE) bottles with polypropylene (PP) caps (foamed polyethylene and pressure sensitive liner). The capsules were subjected to stability testing according to the International Conference on Harmonization guidelines for zone III and IV. The packed containers of prepared capsules along with marketed formulation and bulk α-amylase were kept for accelerated (40±2°C/75±5% relative humidity) and long term (30±2°C/65±5% relative humidity) stability in desiccators with saturated salt solutions for up to 12 months. For accelerated and long term stability, desiccators containing saturated sodium chloride and potassium iodide solutions were kept into ovens at 40°C and 30°C to maintain a constant relative humidity of 74.68±0.13 and 67.98±0.23, respectively. A visual inspection (for discoloration of capsule content), dissolution testing and α-amylase content estimation was carried out every 15 days for the entire period of stability study.

7.2. Carrageenan-Papain Beads

7.2.1. MATERIALS

Hammersten type casein (Himedia Laboratories Pvt. Ltd., Mumbai, India) and trichloroacetic acid (Qualigens Fine Chemicals, Mumbai, India) were used as received. Purified papain, κ-carrageenan, potassium chloride, dibasic sodium phosphate and citric acid were purchased from S. D. Fine-Chem Ltd., Mumbai, India. All the other chemicals and solvents were of analytical grade and were used without further purification. Deionized double-distilled water was used through out the study.

7.2.2. PREPARATION OF BEADS

Concentrated κ-carrageenan solution in distilled water was prepared by heating the powder dispersion at 70°C to get a homogenous solution and cooled to 40°C. The required quantity of enzyme (300 mg papain in 50 ml of final κ-carrageenan solution) was dissolved in a small quantity of water and mixed with concentrated κ-carrageenan solution. The final concentration of κ-carrageenan was adjusted in the range of 2.5-3.5% w/v and was used after being degassed under vacuum. The beads were prepared by dropping the κ-carrageenan solution (10 ml) containing papain from the dropping device, such as syringe with 18G×½" flat-tip hypodermic needle, into a magnetically stirred potassium chloride solution (40 ml) at a rate of 5 ml/min and were allowed to harden for a specific time. Different levels (Table 7.4) of κ-carrageenan, potassium chloride and hardening time were selected. The beads were collected by decanting the potassium

chloride solution, washed with deionized water and dried to a constant weight in a vacuum desiccator (Tarsons Products Pvt. Ltd., Kolkata, India) at room temperature for 48 hours.

Table 7.4: Process variables and their levels for Doehlert shell design.

Factors	Coded levels	Actual levels
A: κ-Carrageenan Concentration (%w/v)	-1	2.50
	-0.5	2.75
	0	3.00
	0.5	3.25
	1	3.50
B: Potassium Chloride Concentration (M)	-0.866	0.33
	-0.577	0.38
	-0.289	0.44
	0	0.50
	0.289	0.56
	0.577	0.62
	0.866	0.67
C: Hardening Time (min)	-0.816	11.84
	0	20.00
	0.816	28.16

7.2.3. EXPERIMENTAL DESIGN

Statistical experimental designs have been in use for several decades.(Plackett and Burman, 1946; Box and Hunter, 1957) These experimental layouts can be adopted at various phases of an optimization process, such as for screening experiments or for finding the optimal conditions for targeted results. Of late, the results analyzed by a statistically planned experiment are better acknowledged than those are carried out by the traditional single variable experiments. Some of the popular choices in statistical design includes the Plackett–Burman design,(Plackett and Burman, 1946) the central composite design, the Box–Behnken design,(Box and Hunter, 1957; Box and Behnken, 1960) uniform shell designs(Doehlert, 1970) and the Graeco–Latin square design. Response

surface methodology has by now been established as a convenient method for developing optimum processes with precise conditions and has also minimized the cost of production of many a process with efficient screening of process parameters.

In order to attain the maximum entrapment and longer T_{90}, three-level full factorial designs can be employed. However, these designs involve a very great number of runs ($N=3^f$, where f is the number of independent variables) compared with the total quadratic coefficients to be determined, m. To alleviate this situation, central composite designs (CCD) can alternatively be used. The introduction of extra runs (star points and centre of design) to augment two-level factorial designs is to estimate the coefficients of the model equation in an efficient way. The number of runs to be made in both orthogonal or rotatable CCD are $N=2^f+2f+1$ (without replications), which is sensibly lower than three level factorial designs. For this reason, CCD are widely used in experimental optimization. However, a more efficient design was devised by Doehlert in 1970,(Doehlert, 1970) who proposed uniform shell designs. These designs being more uniform than any other, show excellent interpolation features. The total number of runs without replication needed for applying Doehlert shell design (DSD) is $N=f^2+f+1$, which is even fewer than in CCD. Thus, DSD leads to the maximum efficiency (ratio between the number of coefficients to be evaluated, m, and the number of runs, N, in the design). For this reason, DSD is highly applied in very different scientific frames.(Vojnovic et al., 1996; Geze et al., 1999; Gustavo Gonzalez and Gonzalez-Arjona, 1999; Voinovich et al., 2000) Before the application of the design, a number of preliminary trials were conducted to determine the conditions at which the process resulted in beads. In the present study the DSD matrix contains 13 points (with $f=3$). To determine the experimental error, the experiment at the centre point was repeated three times at different days. The mean % entrapment, T_{50}, T_{90}, and particle size at the center-replicated points were 76.81±0.50%,

Table 7.5: Distribution of Doehlert shell design experiments in the space of three process variables and results for the measured responses.

Sr. No.	Factors/ levels			Responses				Transformed value		Comp-osite index	Papain in beads	Papain in filtrate	
	κ-carra-geenan (% w/v)	Potassium chloride (M)	Hardening time (min)	% Entrap-ment[a]	T_{50}	T_{90}	Particle size (mm)±SD[b]	% Entrap-ment	T_{90}		Inactive	Active	Inactive
1	0	0	0	76.23	34.05	46.30	1.95±0.19	31.97	23.30	55.26	16.88	5.70	0.52
2	**1**	**0**	**0**	**82.75**	**41.24**	**55.36**	**2.23±0.18**	**48.09**	**40.45**	**88.55**	11.21	4.14	0.35
3	0.5	0.866	0	76.92	43.38	60.40	2.09±0.15	33.67	50.00	83.67	15.47	5.31	0.67
4	-0.5	0.866	0	65.87	36.32	47.15	1.70±0.16	6.34	24.90	31.23	23.89	8.87	0.85
5	-1	0	0	63.31	25.36	35.21	1.68±0.12	0.00	2.29	2.29	25.31	9.54	0.99
6	-0.5	-0.866	0	73.23	24.51	36.12	1.92±0.16	24.55	4.02	28.57	18.74	5.89	0.80
7	0.5	-0.866	0	82.82	33.53	43.32	2.25±0.17	48.28	17.64	65.92	11.68	3.78	0.43
8	0.5	0.289	0.816	78.61	42.58	57.17	1.99±0.12	37.86	43.88	81.74	14.76	4.71	0.51
9	-0.5	0.289	0.816	67.33	34.28	48.55	1.74±0.19	9.93	27.56	37.49	23.20	7.51	0.85
10	0	-0.577	0.816	76.91	34.21	46.73	1.99±0.14	33.64	24.10	57.74	16.40	5.31	0.69
11	0.5	-0.289	-0.816	83.52	32.87	45.81	2.09±0.16	50.00	22.36	72.36	11.70	4.12	0.45
12	-0.5	-0.289	-0.816	73.46	24.85	34.00	1.80±0.14	25.10	0.00	25.10	18.05	6.90	0.56
13	0	0.577	-0.816	76.44	35.67	47.65	1.94±0.13	32.49	25.85	58.34	16.73	5.18	0.64
14	0	0	0	76.93	34.07	43.40	1.89±0.17	33.70	17.80	51.50	15.46	5.08	0.65
15	0	0	0	76.63	33.79	43.90	1.95±0.16	32.96	18.75	51.71	15.66	5.37	0.65
16	0	0	0	77.43	34.12	46.40	1.89±0.19	34.94	23.49	58.42	14.90	5.87	0.68

[a] % Entrapment is the percent active papain in the beads.

[b] SD, standard deviation (n=50).

34.01±0.15 min, 45.00±1.57 min, and 1.92±0.04 mm respectively and showed good reproducibility of the process. The quadratic coefficients were estimated by using the least-squares multiple regression to the observed response. The analysis of variance (ANOVA) was performed in order to determine significance of the fitted equation. All analytical treatments were supported by NCSS software.(Hintze, 2003) The independent factors and their levels used in the study are listed in Table 7.4. The DSD matrix with their coded experimental values and the results of the responses are reported in Table 7.5, while three-dimensional representation of DSD matrix is shown in Figure 7.1. All the experiments were performed in a completely randomized order to exclude any bias.

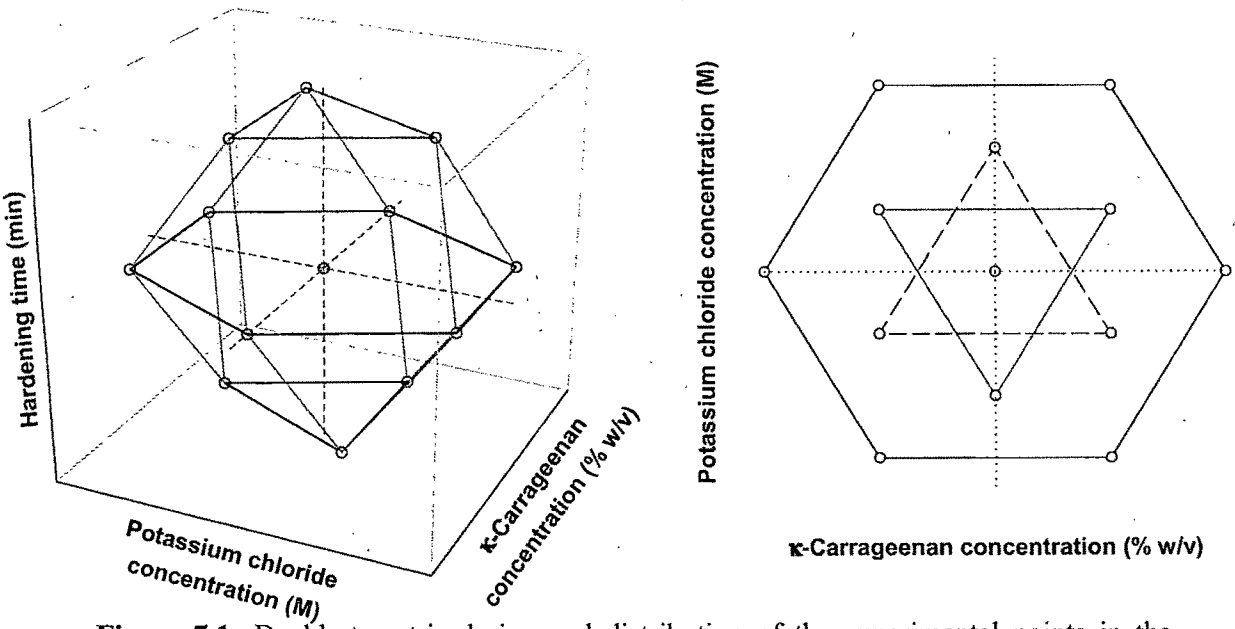

Figure 7.1: Doehlert matrix-design and distribution of the experimental points in the space of three variables. (A) three-dimensional and (B) two-dimensional view.

7.2.4. COMPOSITE INDEX

On completion of the individual experiments, a weighted composite index was used to designate a single score utilizing two responses, i.e., % entrapment, and T_{90}. Many researchers have utilized the technique of multiple responses for optimization studies.

Derringer and Suich illustrated how several response variables can be transformed into one response.(Derringer and Suich, 1980) The applications of one-sided transformations are also demonstrated by different researchers.(Bodeam and Leucata, 1997; Gohel et al., 2003) The application of generalized distance function to incorporate several objectives into a single function has been reported.(Shigeo et al., 1994) As the relative contribution of each individual constraint to the "true" composite score was unknown, a decision was made to assign an arbitrary value of one-half to each of the two response variables.(Taylor et al., 2000) The empirical composite index was devised to yield a score 100 for an optimum result for each of the two responses and each formulations result was transformed to a value between 0 and 50. For % entrapment, highest value (83.52) was assigned a score equal to 50, and lowest value (63.31) was assigned zero score. For T_{90}, lowest value (34.00) was assigned to zero score and the highest value (60.40) was assigned to 50 (see Table 7.5). The batch having a highest composite index would be considered as the batch fulfilling the desired criteria. The raw data transformations were as follows:

Eq. 7.11 $$\text{Transformed value of \% entrapment or } T_{90} = \frac{Y_i - Y_{min}}{Y_{max} - Y_{min}} \times 50$$

where Y_i is the experimental value of individual response variable, Y_{max} and Y_{min} are maximum and minimum values of individual response variable, respectively.

Eq. 7.12 $$\text{Composite index} = \begin{pmatrix}\text{transformed value}\\ \text{of \% entrapment}\end{pmatrix} + \begin{pmatrix}\text{transformed}\\ \text{value of \% } T_{50}\end{pmatrix}$$

7.2.5. CURVE FITTING AND RELEASE MECHANISM

The *'in vitro'* release pattern was evaluated to check the goodness of fit to the zero-order release kinetics (Eq. 7.13), first-order release kinetics(Gibaldi and Feldman, 1967;

Wagner, 1969) (Eq. 7.14), Higuchi's square root of time equation(Higuchi, 1963) (Eq. 7.15), Korsmeyer-Peppas' power law equation(Korsmeyer et al., 1983b; Peppas, 1985) (Eq. 7.16), and Hixson-Crowell's cube root of time equation(Hixson and Crowell, 1931) (Eq. 7.17). The goodness of fit was evaluated by *r* (correlation coefficient) values. For better understanding residual analysis(Pather et al., 1998) of above models was performed on the optimized formulation.

Eq. 7.13 $$Q_t = Q_0 + K_0 t$$

where Q_t is the amount of drug dissolved in time *t*, Q_0 is the initial amount of drug in the solution (most times, Q_0=0), K_0 is the zero order release constant and *t* is release time.

Eq. 7.14 $$Q_t = Q_0 e^{-K_1 t}$$

Where Q_t is the amount of drug dissolved in time *t*, Q_0 is the initial amount of drug in the solution, K_1 is the first order release constant and *t* is release time.

Eq. 7.15 $$Q_t = K_H \sqrt{t}$$

where Q_t is the amount of drug dissolved in time *t*, K_H is the Higuchi dissolution constant and *t* is release time.

Eq. 7.16 $$Q_t / Q_\infty = K_k t^n$$

where Q_t is the amount of drug dissolved in time *t*, Q_∞ is the amount of drug dissolved in ∞ time (the drug loaded in the formulation), Q_t / Q_∞ is the fractional release of the drug in time *t*, K_k is a constant incorporating structural and geometric characteristics of dosage form, *n* is the release (diffusional) exponent that depends on the release mechanism and the shape of the matrix tested(Ritger and Peppas, 1987) and *t* is release time. Interpretation of diffusional exponent is given in Table 7.6.

Eq. 7.17 $$Q_0^{1/3} - Q_t^{1/3} = K_s t$$

where Q_0 is the initial amount of drug in the pharmaceutical dosage form, Q_t is the remaining amount of drug in pharmaceutical dosage form at time t, K_s is a constant incorporating the surface-volume relation and t is release time.

Table 7.6: Interpretation of Korsmeyer-Peppas power law release exponent.

Release exponent (n)	Drug transport mechanism	Rate as a function of time
0.5	Fickian diffusion	$t^{-0.5}$
$0.5<n<1.0$	Anomalous transport	t^{n-1}
1.0	Case-II transport	Zero order release
Higher than 1.0	Super Case-II transport	t^{n-1}

In order to understand the release mechanism, the release data of the optimized batch was fitted to empirical equations proposed by Kopcha(Kopcha et al., 1991) (Eq. 7.18),

Eq. 7.18 $$M = At^{1/2} + Bt$$

In the above equations, M (≤ 70%) is the percentage of drug released at time t, while A and B are, respectively, diffusion and erosion terms. According to this equation, if diffusion and erosion ratio, $A/B=1$, then the release mechanism includes both diffusion and erosion equally. If $A/B>1$, then diffusion prevails, while for $A/B<1$, erosion predominates.

7.2.6. CHARACTERIZATION OF BEADS

7.2.6.1. Estimation of Active Papain

Activity of papain was analyzed with casein according to the modified method of An et al.(An et al., 1994) A reaction mixture containing 5 ml of 1% w/v casein (in 0.05M dibasic sodium phosphate and pH was adjusted to 6.0±0.1 using 0.05M citric acid) was

preincubated at 40°C for 10 min. Different aliquots of enzyme in buffer (pH 6.0±0.1, containing 3.55 g dibasic sodium phosphate, 7.0 g disodium ethylenediaminetetraacetate, and 3.05 g cysteine hydrochloride in 500 ml) and buffer solution was then added, and incubated at 40°C for 60 minutes. The total volume of the reaction mixture, including enzyme, was maintained at 7 ml. The reaction was terminated by adding 3 ml of cold (4°C) 30% w/v trichloroacetic acid (TCA). After allowing unhydrolyzed proteins to precipitate at 4°C for 30 minutes, samples were centrifuged at 5000 rpm for 5 minutes (Remi Instruments Ltd, Mumbai, India). TCA-soluble proteins were recovered in the supernatant and absorbance due to tyrosine content was measured at 280 nm. Blank was prepared separately for each concentration where in the papain was inactivated by adding TCA before the addition of papain. Enzyme activity was expressed as difference of the absorbance between sample and blank at 280 nm (ΔA_{280}).

7.2.6.2. Estimation of Total Papain

An in house fluorescence method was developed for estimation of total papain. Aromatic amino acid residue of papain gives fluorescence which was measured using spectrofluorophotometer (Shimadzu, Model RF-540 with DR-3 data recorder) at emission wavelength of 346 nm. Excitation wavelength, scan speed and sensitivity were fixed at 257 nm, 3 (slow) and 5 (16X) respectively. Method was found to be linear over an analytical range of 5-150 µg/ml. Difference between the results of modified An et al.(An et al., 1994) method and fluorescence method gives an inactive papain fraction.

7.2.6.3. Determination of Entrapment Efficiency

Entrapment efficiency was determined by dissolving the enzyme-loaded beads in a magnetically stirred (500 rpm) simulated gastric fluid (SGF) without enzyme (USP XXVI) at room temperature for about 90 min. An aliquot of 2 ml was taken and neutralized to pH 6.0±0.1 using 0.01 N sodium hydroxide or hydrochloric acid. The resulting solution was centrifuged at 2500 rpm for 10 min (Remi Instruments Ltd, Mumbai, India) and supernatant was assayed (n=3) for active and total enzyme content by modified An et al.(An et al., 1994) method and fluorescence method respectively. Entrapment efficiency was calculated as:

$$\text{Entrapment efficiency} = \frac{\text{Enzyme loaded (active papain fraction in beads)}}{\text{Theoretical enzyme loading}} \times 100 \quad (9)$$

Un-entrapped active and total papain content were determined from the filtrate using above methods.

7.2.6.4. 'In vitro' Dissolution and Determination of T_{50} and T_{90}

For optimization purposes, dissolution study of all batches was carried out in 500 ml of SGF without enzyme using the USP XXVI dissolution apparatus 2 (TDT-60T, Electrolab, Mumbai, India) at 37±0.5 °C with paddle speed of 75 rpm. For estimation of active and inactive papain release, beads equivalent to 40 mg of theoretically loaded papain (n=3) were subjected to *'in. vitro'* dissolution study and aliquots of 2 ml were collected, neutralized to pH 6.0±0.1 using 0.01 N sodium hydroxide or hydrochloric acid, and suitable volume was assayed at 0, 5, 10, 15, 20, 30, 45, 60, 90 and 120 min. Time required for 50 (T_{50}) and 90 (T_{90}) percent of enzyme release were used to evaluate the onset and duration of action respectively. For determination of T_{50} and T_{90}, accurately

weighed samples (n=3) equivalent to about 40 mg of practically entrapped active fraction of papain (as % label claim) were subjected to dissolution and processed as above. T_{50} and T_{90} were found by extrapolating the % label claim versus time plot.

7.2.6.5. Particle Size Measurements

The particle sizes of 50 gel beads were measured with a micrometer for each formulation and the mean particle size was determined.

7.2.6.6. Effect of pH on Release Profile

To study the effect of pH on papain release profile, *'in vitro'* dissolution study was carried out as before using 500 ml of different pH media (SGF without enzyme pH 1.2, phosphate buffer pH 4.0, simulated intestinal fluid (SIF) without enzyme pH 6.8, phosphate buffer pH 7.4, and phosphate buffer pH 8.0) on the optimized batch. Accurately weighed samples (n=3) equivalent to about 40 mg of papain were introduced to dissolution media and samples of 2 ml were collected at 0, 0.25, 0.50, 0.75, 1.0, 1.5, 2.0, 2.5, 3.0, 3.5, 4.0, 4.5, 5.0, 5.5 and 6.0 hr. Samples were neutralized to pH 6.0±0.1 using 0.01 N sodium hydroxide or hydrochloric acid and assayed for enzyme content as before.

7.2.6.7. Fourier Transform Infra-Red Spectroscopy (FTIR)

IR transmission spectra were obtained using a FTIR spectrophotometer (FTIR-8300, Shimadzu, Japan). A total of 2% (w/w) of sample, with respect to the potassium bromide

(KBr; S. D. Fine Chem Ltd., Mumbai, India) disc, was mixed with dry KBr. The mixture was ground into a fine powder using an agate mortar before compressing into KBr disc under a hydraulic press at 10,000 psi. Each KBr disc was scanned 16 times at 4 mm/s at a resolution of 2 cm^{-1} over a wavenumber region of 400–4000 cm^{-1} using Happ-Genzel apodization. The characteristic peaks were recorded.

7.2.6.8. Differential Scanning Calorimetry (DSC)

Differential scanning calorimetric analysis was used to characterize the thermal behavior of the isolated substances, empty beads, enzyme-loaded beads, and physical mixture of papain: blank beads (1:6.21, same as that of the optimized formulation). DSC thermograms were obtained using an automatic thermal analyzer system (DSC-60, Shimadzu, Japan). Temperature calibration was performed using indium as a standard. Samples were crimped in a standard aluminum pan and heated from 40–400 °C at a heating rate of 10 °C/min under constant purging of dry nitrogen at 30 ml/min. An empty pan, sealed in the same way as the sample, was used as a reference.

7.2.6.9. Scanning Electron Microscopy (SEM)

The purpose of SEM study was to obtain a topographical characterization of beads. The beads were mounted on brass stubs using carbon paste. SEM photographs were taken with scanning electron microscope (JSM-5610LV, Jeol Ltd., Tokyo, Japan) at the required magnification at room temperature. The working distance of 39 mm was maintained and acceleration voltage used was 5 kV, with the secondary electron image (SEI) as a detector.

7.2.7. PREPARATION OF CAPSULE FORMULATION, PACKAGING, AND STABILITY STUDY

Accurately weighed carrageenan beads equivalent to 40 mg of papain were filled into a hard gelatin capsule manually. The joint of the capsule body and cap was carefully sealed by pressing them to fit in the lock mechanism. The capsules were packed in high density polyethylene (HDPE) bottles with polypropylene (PP) caps (foamed polyethylene and pressure sensitive liner). The capsules were subjected to stability testing according to the International Conference on Harmonization guidelines for zone III and IV. The packed containers of prepared capsules along with marketed formulation and bulk papain were kept for accelerated (40±2°C/75±5% relative humidity) and long term (30±2°C/65±5% relative humidity) stability in desiccators with saturated salt solution for up to 12 months. A visual inspection (for discoloration of capsule content), dissolution testing, and papain content estimation was carried out every 15 days for the entire period of stability study.

7.3. Carrageenan-Pepsin Beads

7.3.1. MATERIALS

Bovine hemoglobin powder (Himedia Laboratories Pvt. Ltd., Mumbai, India) and trichloroacetic acid (TCA), hydrochloric acid (HCl), and potassium bromide (KBr, IR grade) (Qualigens Fine Chemicals, Mumbai, India) were used as received. Purified pepsin, κ-carrageenan, potassium chloride, sodium hydroxide (NaOH), phosphomolybdotungstic reagent, and citric acid were purchased from S. D. Fine-Chem Ltd., Mumbai, India. All the other chemicals and solvents were of analytical grade and were used without further purification. Deionized double-distilled water was used through out the study.

7.3.2. PREPARATION OF BEADS

Concentrated κ-carrageenan solution in distilled water was prepared by heating the powder dispersion at 70°C to get homogenous solution and cooled to 40°C. Required quantity of enzyme (200 mg pepsin in 50 ml of final κ-carrageenan solution) was dissolved in small quantity of water and mixed with concentrated κ-carrageenan solution. Final concentration of κ-carrageenan was adjusted in the range of 2.5-3.5% w/v and was used after being degassed under a vacuum. The beads were prepared by dropping the κ-carrageenan solution (10 ml) containing pepsin from the dropping device such as syringe with 18G×½" flat-tip hypodermic needle to a magnetically stirred potassium chloride solution (40 ml) at a rate of 5 ml/min and were allowed to harden for specific time.

Different levels of independent factors (κ-carrageenan, potassium chloride and hardening time) and the dependent responses (% entrapment, T_{50}, T_{90}, and particle size)used in the study are listed in Table 7.7. The beads were collected by decanting potassium chloride solution, washed with deionized water and dried to a constant weight in vacuum desiccator (Tarsons Products Pvt. Ltd., Kolkata, India) at room temperature for 48 hours.

Table 7.7: Process variables and responses with constraints for Box-Behnken Design.

Factors	Coded levels	Actual levels
A: κ-Carrageenan Concentration (%w/v)	-1	2.50
	0	3.00
	1	3.50
B: Potassium Chloride Concentration (M)	-1	0.3
	0	0.5
	1	0.7
C: Hardening Time (min)	-1	10
	0	20
	1	30
Responses	Constraint	
M_1: % Entrpament	>80%	
M_2: T_{50} (min)	–	
M_3: T_{90} (min)	<40 min	
M_4: Particle size (mm)	–	

7.3.3. BOX-BEHNKEN DESIGN

Box-Behnken designs (BBD) are response surface methods for a spherical domain whose most interesting property is that each factor takes only 3 levels (Box and Behnken, 1960; Lewis et al., 1999). Each combination of the extreme values of two of the variables is tested, the remaining variables taking a coded level of zero. BBD is a spherical design, with all points lying on a sphere of radius $\sqrt{2}$ and on the centre of the edge of a cube (Figure 7.2). Also, the Box-Behnken design does not contain any points at the vertices of the cubic region created by the upper and lower limits for each variable. Its geometry is the same as that of the 3 factor Doehlert design, but in a different orientation (Hileman et

al., 1993). Another advantageous property of the Box-Behnken design is that inflation factors are normally low (1.01 for the present matrix), provided sufficient centre points are added. The estimators are thus nearly independent, and the matrix nearly orthogonal.

In order to attain the optimum response, three-level full factorial designs can be employed. However, these designs involve a very great number of runs ($N=3^f$, where f is the number of the independent variables) compared with the total quadratic coefficients to be determined, m. To alleviate this situation, central composite designs (CCD) can alternatively be used. The introduction of extra runs (star points and centre of design) to augment two-level factorial designs is to estimate the coefficients of the model equation in an efficient way. The number of runs to be made in both orthogonal or rotatable CCD are $N=2^f+2f+1$ (without replications), sensibly lower than three level factorial designs. For this reason, CCD are widely used in experimental optimization. However, a more efficient design was devised by Box and Behnken (Box and Behnken, 1960), who proposed some new three level desings for the study of quantitative variables. These designs being more uniform than any other, show excellent interpolation features. The total number of runs without replication needed for applying BBD is 13, even lesser than in CCD. Thus, BBD lead to the maximum efficiency (ratio between the number of coefficients to be evaluated, m, and the number of runs, N, in the design). CCD usually has axial points outside the 'cube' (unless alpha, the axial spacing needed to ensure orthogonality, is specified as less than or equal to one). BBD do not have axial points, thus all design points fall within the safe operating zone. BBD also ensure that all factors are never set at their high levels, simultaneously (Box and Behnken, 1960). Also, each factor requires only three levels instead of the five required for CCD (unless alpha is equal to one), which may be experimentally more convenient and less expensive to run than CCD with the same number of factors. For this reason, BBD are highly applied in

very different scientific frames (Bodea and Leucuta, 1998; Ragonese et al., 2002; Rana et al., 2004; Turner et al., 2004; Bae and Shoda, 2005).

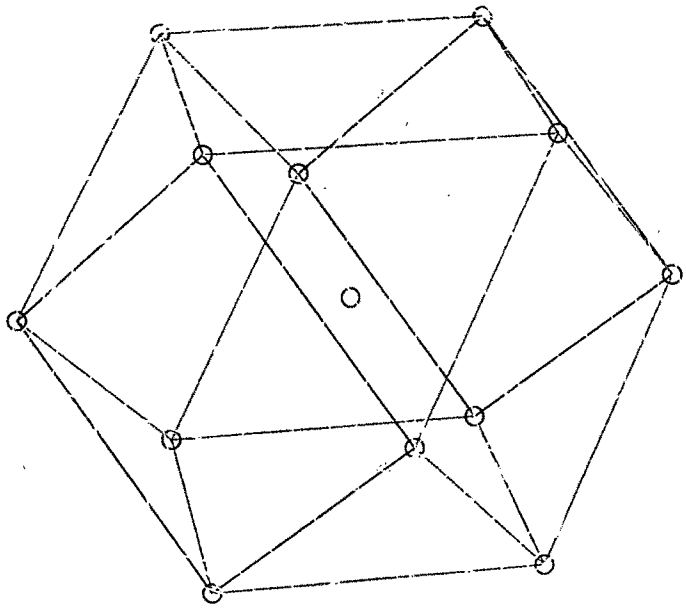

Figure 7.2: Three-dimensional view of Box-Behnken design.

Before the application of the design, number of preliminary trials were conducted to determine the conditions at which the process resulted to beads. In the present study the BBD matrix contains 13 points (with f=3). To determine the experimental error, the experiment at the centre point was repeated three times at different days. The mean % entrapment, T_{50}, T_{90}, and particle size at the center-replicated points were 76.86±0.21%, 33.82±0.22 min, 44.09±0.32 min, and 1.93±0.04 mm respectively and showed good reproducibility of the process. For predicting the optimal region, a second order polynomial function was fitted to correlate relationship between variables and responses. The behavior of the system was explained by the following quadratic equation:

Eq. 7.19
$$Y = \beta_0 + \sum \beta_i x_i + \sum \beta_{ij} x_i x_j + \sum \beta_{ii} x_i^2$$

where Y is predicted response, β_0 is offset term (model constant), β_i is linear offset, β_{ii} is squared offset, β_{ij} is interaction effect, and x_i is dimensionless coded value of independent

variables (X_i). From the quadratic equation, response surfaces were generated and the overlapping region of the responses with constraint was considered as the optimum region where the beads with desired criteria can be produced. The analysis of variance (ANOVA) was performed in order to determine significance of the fitted equation. All analytical treatments were supported by NCSS software (Hintze, 2003). The quality of fit of the polynomial model equation was expressed by the adjusted coefficient of determination R^2_{adj}. All experimental designs were randomized to exclude any bias. The process variables with their coded experimental values and the results of the responses are reported in Table 7.8, while the design is also shown geometrically in Figure 7.2.

Table 7.8: Matrix of Box-Behnken Design and results for the measured responses.

Factors/ levels				Responses			
ES[a]	κ-carrageenan (% w/v)	Potassium chloride (M)	Hardening time (min)	% Entra-pment	T_{50} (min)	T_{90} (min)	Particle size (mm)
5	-1	-1	0	64.90	19.20	29.70	1.833
11	1	-1	0	84.80	35.90	49.30	2.363
2	-1	1	0	57.48	32.65	46.10	1.646
14	1	1	0	77.85	48.30	67.80	2.209
7	-1	0	-1	66.06	22.30	32.50	1.708
9	1	0	-1	85.70	38.47	51.90	2.325
1	-1	0	1	60.47	29.10	44.10	1.661
12	1	0	1	81.69	45.50	62.00	2.195
3	**0**	**-1**	**-1**	**81.41**	**24.50**	**35.30**	**2.111**
6	0	-1	1	77.20	33.05	46.05	2.054
15	0	1	-1	73.81	37.86	50.83	1.857
8	0	1	1	69.32	44.60	62.95	1.809
13	0	0	0	77.03	33.70	44.15	1.951
4	0	0	0	76.93	34.07	43.74	1.888
10	0	0	0	76.63	33.69	44.38	1.948

[a] ES, experimental sequence.

7.3.4. CURVE FITTING

The *'in vitro'* release pattern was evaluated to check the goodness of fit to the zero-order release kinetics (Eq. 7.20), first-order release kinetics (Gibaldi and Feldman, 1967;

Wagner, 1969) (Eq. 7.21), Higuchi's square root of time equation (Higuchi, 1963) (Eq. 7.22), Korsmeyer-Peppas' power law equation (Korsmeyer et al., 1983b; Peppas, 1985) (Eq. 7.23), and Hixson-Crowell's cube root of time equation (Hixson and Crowell, 1931) (Eq. 7.24). The goodness of fit was evaluated by *r* (correlation coefficient) values. For better understanding residual analysis (Pather et al., 1998) of above models was performed on the optimized formulation.

Eq. 7.20 $$Q_t = Q_0 + K_0 t$$

where Q_t is the amount of drug dissolved in time *t*, Q_0 is the initial amount of drug in the solution (most times, Q_0=0), K_0 is the zero order release constant and *t* is release time.

Eq. 7.21 $$Q_t = Q_0 e^{-K_1 t}$$

Where Q_t is the amount of drug dissolved in time *t*, Q_0 is the initial amount of drug in the solution, K_1 is the first order release constant and *t* is release time.

Eq. 7.22 $$Q_t = K_H \sqrt{t}$$

where Q_t is the amount of drug dissolved in time *t*, Q_H is the Higuchi dissolution constant and *t* is release time.

Eq. 7.23 $$Q_t / Q_\infty = K_k t^n$$

where Q_t is the amount of drug dissolved in time *t*, Q_∞ is the amount of drug dissolved in ∞ time (the drug loaded in the formulation), Q_t / Q_∞ is the fractional release of the drug in time *t*, K_k is a constant incorporating structural and geometric characteristic of dosage form, *n* is the release (diffusional) exponent that depends on the release mechanism and the shape of the matrix tested (Ritger and Peppas, 1987) and *t* is release time. Interpretation of diffusional exponent is given in Table 7.9.

Table 7.9: Interpretation of Korsmeyer-Peppas power law release exponent.

Release exponent (n)	Drug transport mechanism	Rate as a function of time
0.5	Fickian diffusion	$t^{-0.5}$
$0.5<n<1.0$	Anomalous transport	t^{n-1}
1.0	Case-II transport	Zero order release
Higher than 1.0	Super Case-II transport	t^{n-1}

Eq. 7.24 $$Q_0^{1/3} - Q_t^{1/3} = K_s t$$

where Q_0 is the initial amount of drug in the pharmaceutical dosage form, Q_t is the remaining amount of drug in pharmaceutical dosage form at time t, K_s is a constant incorporating the surface-volume relation and t is release time.

In order to understand the release mechanism, the release data of the optimized batch was fitted to empirical equations proposed by Kopcha (Kopcha et al., 1991) (Eq. 7.25),

Eq. 7.25 $$M = At^{1/2} + Bt$$

In the above equations, M ($\leq$ 70%) is the percentage of drug released at time t, while A and B are, respectively, diffusion and erosion terms. According to this equation, if diffusion and erosion ratio, $A/B=1$, then the release mechanism includes both diffusion and erosion equally. If $A/B>1$, then diffusion prevails, while for $A/B<1$, erosion predominates.

7.3.5. CHARACTERIZATION OF BEADS

7.3.5.1. Estimation of Pepsin

The activity of pepsin was measured by the modified method of Anson (Anson, 1939) wherein the quantity of peptides, non-precipitable by TCA was determined and assayed using the phosphomolybdotungstic reagent. To prepare the 2.0% (w/v) hemoglobin

substrate solution, 2.5 g of hemoglobin was dissolved in 100 mL of distilled water and mixed vigorously, and then filtered with a glass wool filter. Before assay, 80 mL of filtrate was mixed with 20 ml of 0.3 M HCl. Properly diluted enzyme solution (1.0 ml) was added to 5.0 ml of the above substrate solution which had been equilibrated in a 37°C water bath for 20 min, mixed and incubated at 37°C for exactly 10 min, and then 10 ml of 5% w/v TCA was added and mixed vigorously for 1 min by a vortex. The resultant mixture was filtered twice through the same filter paper previously washed with 5% w/v TCA, then with water and dried. First 5 ml of filtrate was discarded and 3 ml of the above filtrate was transferred to a flask containing 20 ml of water. Then, 1 ml of 20% w/v NaOH and 1 ml of phosphomolybdotungstic reagent were added, and was allowed to stand for 15 min for full color development. The absorbance of the resultant solution was measured at 540 nm (UV-1601, Shimadzu, Japan) at room temperature. The blank was prepared according to the above procedure, except TCA solution was added before the enzyme solution.

7.3.5.2. Determination of Entrapment Efficiency

Entrapment efficiency was determined by dissolving the enzyme loaded beads in a magnetically stirred simulated gastric fluid (SGF) without enzyme (USP XXVI) for about 90 min. The resulting solution was centrifuged at 2500 rpm for 10 min (Remi Instruments Ltd, Mumbai, India) and supernatant was assayed (n=3) for enzyme content by above method. Entrapment efficiency was calculated as:

Eq. 7.26

$$\text{Entrapment efficiency} = \frac{\text{Enzyme loaded}}{\text{Theoratical enzyme loading}} \times 100$$

7.3.5.3. Determination of T_{50} and T_{90}

Time required for 50 (T_{50}) and 90 (T_{90}) percent of enzyme release were used to evaluate the onset and duration of action respectively. For optimization purpose, dissolution study of all batches was carried out in 500 ml of SGF without enzyme using the USP XXVI dissolution apparatus 2 (TDT-60T, Electrolab, Mumbai, India) at 37±0.5 °C with paddle speed of 75 rpm. Accurately weighed samples (n=3) equivalent to about 20 mg of pepsin were subjected to dissolution, aliquots of 2 ml were collected, and assayed at 0, 5, 10, 15, 20, 30, 45, 60, 90 and 120 min. T_{50} and T_{90} were found by extrapolating the % enzyme released versus time plot.

7.3.5.4. Particle Size Measurements

The particle sizes of 50 gel beads were measured with a micrometer for each formulation and the mean particle size was determined.

7.3.5.5. Effect of pH on Release Profile

To study the effect of pH on pepsin release profile, *'in vitro'* dissolution study was carried out as before using 500 ml of different pH media (SGF without enzyme pH 1.2, phosphate buffer pH 4.0, simulated intestinal fluid (SIF) without enzyme pH 6.8, phosphate buffer pH 7.4, and phosphate buffer pH 8.0) on the optimized batch. Accurately weighed samples (n=3) equivalent to about 20 mg of pepsin were introduced to dissolution media and samples of 2 ml were collected at 0, 0.25, 0.50, 0.75, 1.0, 1.5,

2.0, 2.5, 3.0, 3.5, 4.0, 4.5, 5.0, 5.5 and 6.0 hr. Samples were filtered through whatman® filter paper #42 and assayed for enzyme content as before.

7.3.5.6. Fourier Transform Infra-Red Spectroscopy (FTIR)

IR transmission spectra were obtained using a FTIR spectrophotometer (FTIR-8300, Shimadzu, Japan). A total of 2% (w/w) of sample, with respect to the potassium bromide (KBr; S. D. Fine Chem Ltd., Mumbai, India) disc, was mixed with dry KBr. The mixture was ground into a fine powder using an agate mortar before compressing into KBr disc under a hydraulic press at 10,000 psi. Each KBr disc was scanned at 4 mm/s at a resolution of 2 cm over a wavenumber region of 400–4000 cm^{-1}. The characteristic peaks were recorded.

7.3.5.7. Differential Scanning Calorimetry (DSC)

Differential scanning calorimetric analysis was used to characterize the thermal behavior of the isolated substances, empty and enzyme loaded beads. DSC thermograms were obtained using an automatic thermal analyzer system (DSC-60, Shimadzu, Japan). Temperature calibration was performed using indium as a standard. Samples were crimped in a standard aluminum pan and heated from 40–400 °C at a heating rate of 10 °C/min under constant purging of dry nitrogen at 30 ml/min. An empty pan, sealed in the same way as the sample, was used as a reference.

7.3.5.8. Scanning Electron Microscopy (SEM)

The purpose of SEM study was to obtain a topographical characterization of beads. The beads were mounted on brass stubs using carbon paste. SEM photographs were taken with scanning electron microscope (JSM-5610LV, Jeol Ltd., Tokyo, Japan) at the required magnification at room temperature. The working distance of 39 mm was maintained and acceleration voltage used was 5 kV, with the secondary electron image (SEI) as a detector.

7.3.6. PREPARATION OF CAPSULE FORMULATION, PACKAGING, AND STABILITY STUDY

Accurately weighed carrageenan beads equivalent to 20 mg of pepsin were filled into a hard gelatin capsule manually. The joint of the capsule body and cap was carefully sealed by pressing them to fit in the lock mechanism. The capsules were packed in high density polyethylene (HDPE) bottles with polypropylene (PP) caps (foamed polyethylene and pressure sensitive liner). The capsules were subjected to stability testing according to the International Conference on Harmonization guidelines for zone III and IV. The packed containers of prepared capsules along with marketed formulation and bulk pepsin were kept for accelerated (40±2°C/75±5% relative humidity) and long term (30±2°C/65±5% relative humidity) stability in desiccators with saturated salt solution for up to 12 months. A visual inspection (for discoloration of capsule content), dissolution testing, and pepsin content estimation was carried out every 15 days for the entire period of stability study.

7.4. References

AN, H., SEYMOUR, T. A., WU, J. W. and MORRISSEY, M. T., 1994. Assay systems and characterization of Pacific whiting (*Merluccius productus*) protease. J. Food Sci. 59, 277-281.

ANSON, M. L., 1939. The estimation of pepsin, trypsin, papain and cathepsin with hemoglobin. J. Gen. Physiol. 22, 79-89.

BAE, S. and SHODA, M., 2005. Statistical optimization of culture conditions for bacterial cellulose production using Box-Behnken design. Biotechnol Bioeng 90, 20-28.

BODEA, A. and LEUCUTA, S. E., 1998. Optimization of propanolol hydrochloride susained-release pollets using Box-Behnken desing and desirability function. Drug Dev. Ind. Pharm. 24, 145-155.

BODEAM, X. and LEUCATA, S. E., 1997. Optimization of hydrophilic matrix tablets using a D-optimal design. Int. J. Pharm. 153, 247-255.

BOX, G. E. P. and BEHNKEN, D. W., 1960. Some new three level desings for the study of quantitative variables. Technometrics 2, 455-476.

BOX, G. E. P. and HUNTER, J. S., 1957. Multi-factorial designs for exploring response surfaces. Ann. Math. Stat. 28, 195-241.

DERRINGER, G. and SUICH, R., 1980. Simultaneous optimization of several responses variables. J. Qual. Technol. 2, 214-219.

DOEHLERT, D.H., 1970. Uniform shell designs. Appl. Stat. 19, 231-239.

GEZE, A., VENIER-JULIENNE, M. C., MATHIEU, D., FILMON, R., PHAN-TAN-LUU, R. and BENOIT, J. P., 1999. Development of 5-iodo-2'-deoxyuridine milling process to reduce initial burst release from PLGA microparticles. Int. J. Pharm. 178, 257-268.

GIBALDI, M. and FELDMAN, S., 1967. Establishment of sink conditions in dissolution rate determinations - theoretical considerations and application to non-disintegrating dosage forms. J. Pharm. Sci. 56, 1238-1242.

GOHEL, M. C., PATEL, M. M. and AMIN, A. F., 2003. Development of modified release diltiazem HCl tablets using composite index to identify optimal formulation. Drug Dev. Ind. Pharm. 29, 565-574.

GUSTAVO GONZALEZ, A. and GONZALEZ-ARJONA, DOMINGO, 1999. Computational program for evaluating and optimizing response-surface curves based on uniform shell designs. Talanta 49, 433-439.

HIGUCHI, T., 1963. Mechanism of sustained-action medication. Theoretical analysis of rate of release of solid drugs dispersed in solid matrices. J. Pharm. Sci. 52, 1145-1149.

HILEMAN, G. A., GOSKONDA, S. R., SPALITTO, A. J. and UPADRASHA, S. M., 1993. Response surface optimization of high dose pellets by extrusion and spheronization. Int. J. Pharm. 100, 71-79.

HINTZE, J., NCSS and PASS ver. 2003, *Number Cruncher Statistical Systems*, Kaysville, Utah, www.ncss.com, 2003.

HIXSON, A.W. and CROWELL, J.H., 1931. Dependence of reaction velocity upon surface and agitation. Ind. Eng. Chem. 23, 923-931.

HSIU, JULIA, FISCHER, EDMOND H. and STEIN, ERIC A., 1964. Alpha-amylase as calcium-metalloenzymes. II. Calcium and the catalytic activity. Biochemistry 3, 61-66.

KOPCHA, M., LORDI, N. and TOJO, K.J., 1991. Evaluation of release from selected thermosoftening vehicles. J. Pharm. Pharmacol. 43, 382-387.

KORSMEYER, R. W., GURNY, R., DOELKER, E. M., BURI, P. and PEPPAS, N. A., 1983a. Mechanism of solute release from porous hydrophilic polymers. Int. J. Pharm. 15, 25-35.

KORSMEYER, R.W., GURNY, R., DOELKER, E.M., BURI, P. and PEPPAS, N.A., 1983b. Mecanism of solute release from porous hydrophilic polymers. Int. J. Pharm. 15, 25-35.

LEWIS, GARETH A., MATHIEU, DIDIER and PHAN-TAN-LUU, R., 1999. Response surface methodology. in: Pharmaceutical Experimental Design, Drugs and The Pharmaceutical Sciences, Vol. 92, Marcel Dekker, Inc., New York, pp. 185-246.

PATHER, S. INDIRAN, RUSSELL, IRINA, SYCE, JAMES A. and NEAU, STEVEN H., 1998. Sustained release theophylline tablets by direct compression Part 1: formulation and in vitro testing. Int. J. Pharm. 164, 1-10.

PEPPAS, N.A., 1985. Analysis of Fickian and non-Fickian drug release from polymers. Pharm. Acta Helv. 60, 110-111.

PLACKETT, R. L. and BURMAN, J. P., 1946. The design of optimum multifactorial experiments. Biometrika 33, 305-325.

RAGONESE, R., MACKA, M., HUGHES, J. and PETOCZ, P., 2002. The use of the Box-Behnken experimental design in the optimisation and robustness testing of a capillary electrophoresis method for the analysis of ethambutol hydrochloride in a pharmaceutical formulation. J Pharm Biomed Anal 27, 995-1007.

RANA, P., MOHAN, N. and RAJAGOPAL, C., 2004. Electrochemical removal of chromium from wastewater by using carbon aerogel electrodes. Water Res 38, 2811-2820.

RICE, EUGENE W., 1959. Improved spectrophotometric determination of amylase with a new stable starch substrate solution. Clin. Chem. 5, 592-596.

RITGER, P. L. and PEPPAS, N. A., 1987. A simple equation for description of solute release II. Fickian and anomalous release from swellable devices. J. Controlled Release 5, 37-42.

SHIGEO, O., TOSHIHIKO, K., YOUSUKE, M., HOROSHIMA, S., KOZO, T. and NAGAI, T., 1994. A new attempt to solve the scale up problem for granulation using response surface methodology. J. Pharm. Sci. 83, 439-443.

SMITH, BENJAMIN W. and ROE, JOSEPH H., 1957. A micromodification of the Smith and Roe method for the determination of amylase in body fluids. J. Biol. Chem. 227, 357-362.

TAYLOR, MICHAEL K., GINSBURG, JERI, HICKEY, ANTHONY J. and GHEYAS, FERDOUS, 2000. Composite method to quantify powder flow as a screening method in early tablet or capsule formulation development. AAPS PharmSciTech 1, article 18 (www.pharmascitech.com).

TURNER, C., WHITEHAND, L. C., NGUYEN, T. and MCKEON, T., 2004. Optimization of a supercritical fluid extraction/reaction methodology for the analysis of castor oil using experimental design. J Agric Food Chem 52, 26-32.

VOINOVICH, D., MONEGHINI, M., PERISSUTTI, B., FILIPOVIC-GRCIC, J. and GRABNAR, I., 2000. Preparation in high-shear mixer of sustained-release pellets by melt pelletisation. Int. J. Pharm. 203, 235-244.

VOJNOVIC, D., CHICOO, D. and ZENARY, H. EL., 1996. Doehlert experimental design applied to optimization and quality control of a granulation process in a high shear mixer. Int. J. Pharm. 145, 203-213.

WAGNER, J. G., 1969. Interpretation of percent dissolved-time plots derived from in vitro testing of conventional tablets and capsules. J. Pharm. Sci. 58, 1253-1257.